Supplementary Materials

Structural Diversity of the Oxovanadium Organodiphosphonate System: A Platform for the Design of Void Channels**

Wayne Ouellette, Ming Hui Yu, Charles J. O'Connor, and Jon Zubieta

1. TGA profiles.
2. IR data for **6c** and **6c'**.
3. Magnetic susceptibility plots.

$[V_2O_2(H_2O)\{O_3P(CH_2)_2PO_3\}]\cdot 1H_2O$ (1a·1H_2O)

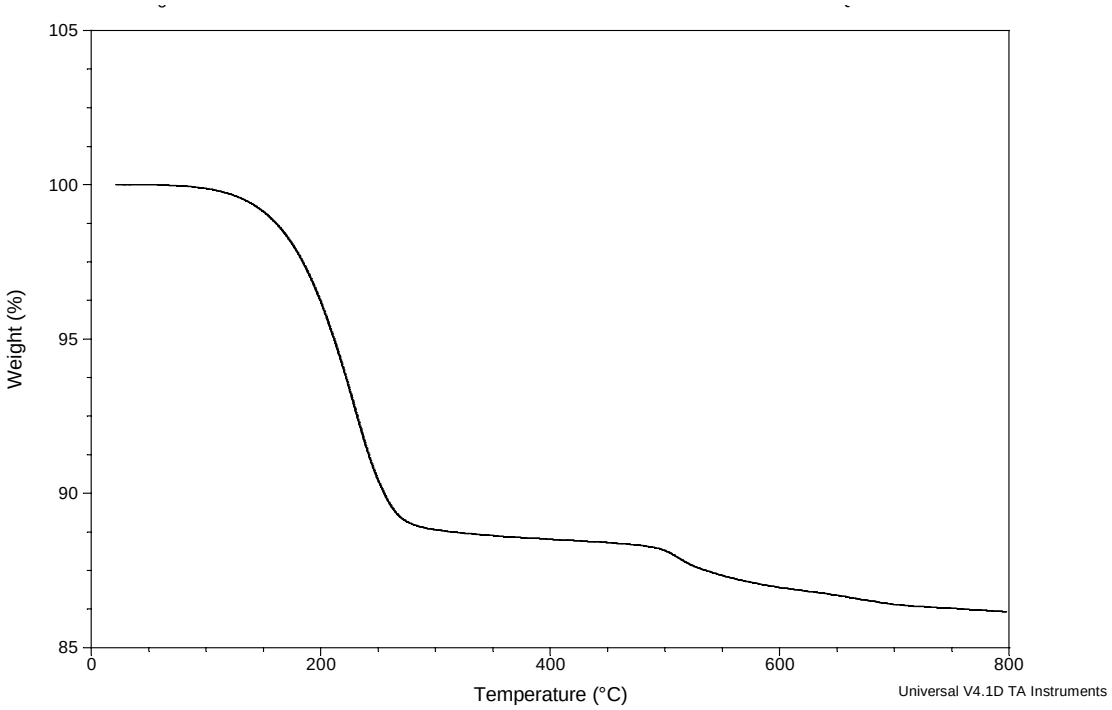

$[V_2O_2(H_2O)\{O_3P(CH_2)_3PO_3\}]\cdot 2H_2O$ (1b·2H_2O)

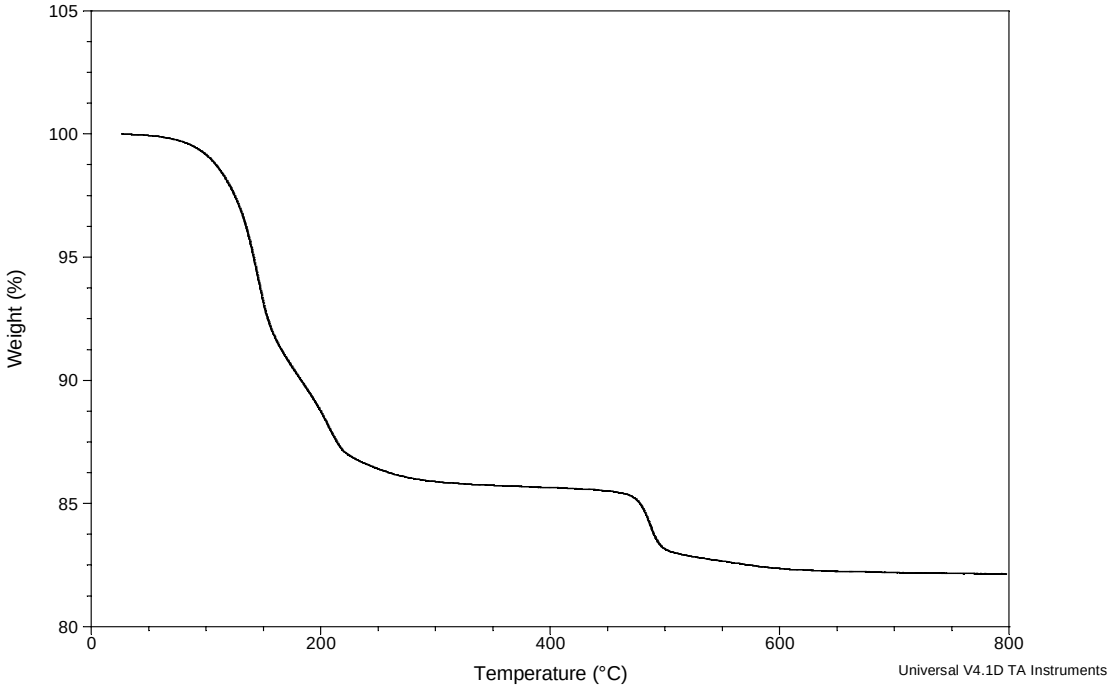

$[V_2O_2(H_2O)\{O_3P(CH_2)_4PO_3\}]\cdot 3H_2O$ (1c·$3H_2O$)

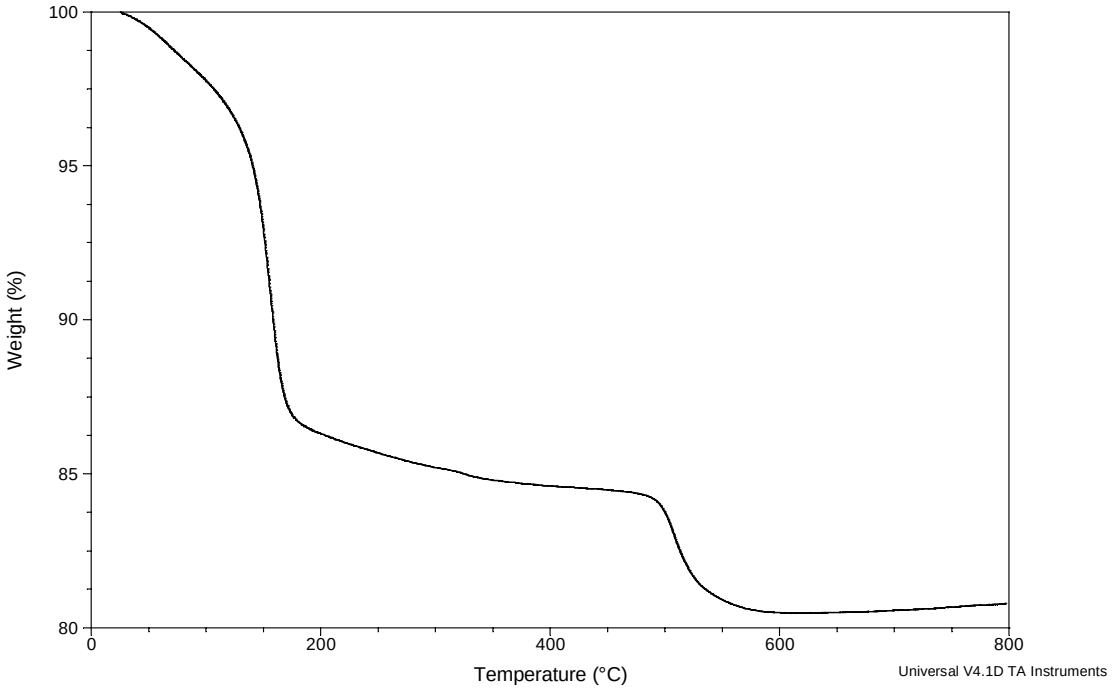

$[V_2O_2(H_2O)\{O_3P(CH_2)_5PO_3\}]\cdot 3H_2O$ (1d·$3H_2O$)

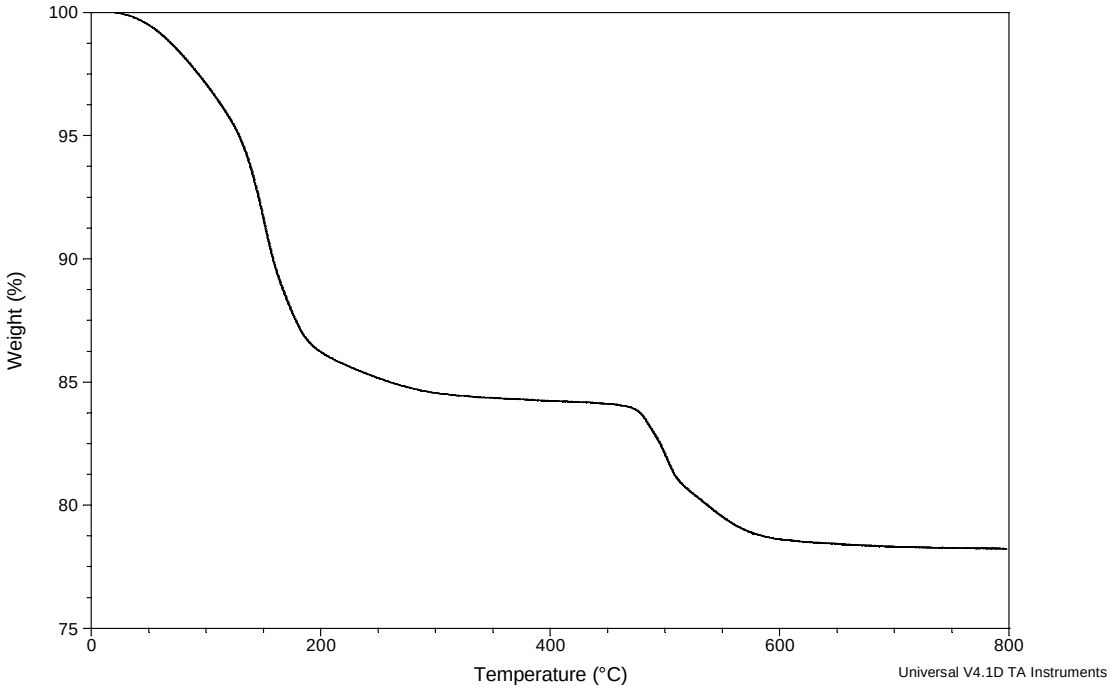

$[NH_3(CH_2)_2NH_3][V_4O_4(OH)_2\{O_3P(CH_2)_3PO_3\}_2]\bullet 4H_2O$ ($4a\cdot 4H_2O$)

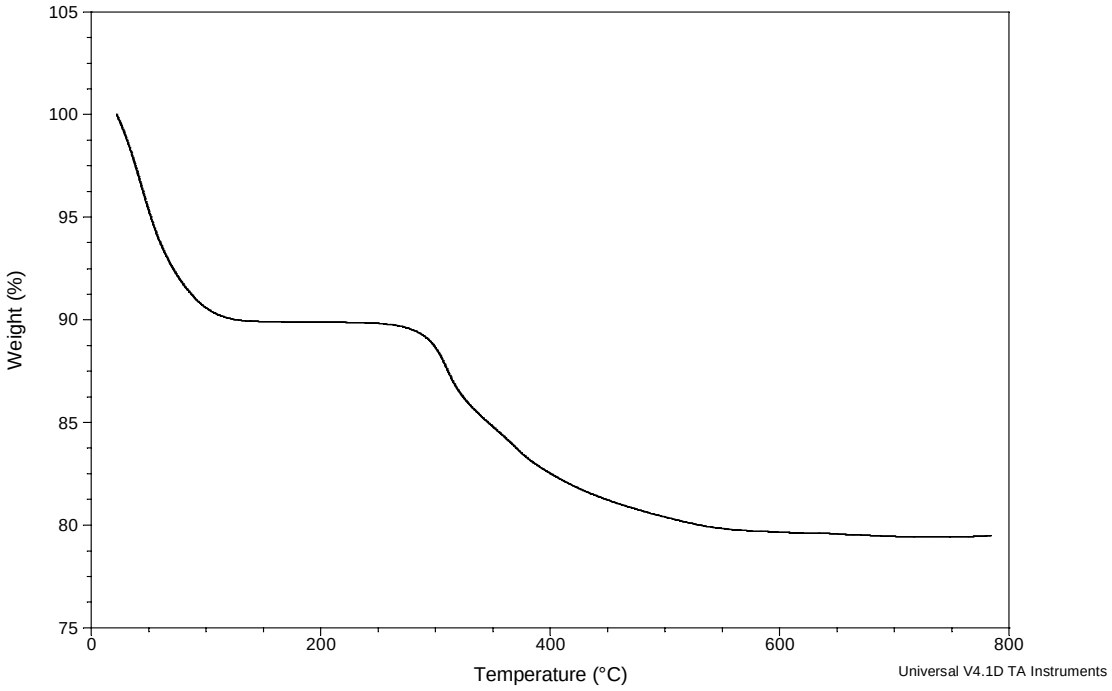

$[NH_3(CH_2)_3NH_3][V_4O_4(OH)_2\{O_3P(CH_2)_3PO_3\}_2]\bullet 3H_2O$ ($4b\cdot 3H_2O$)

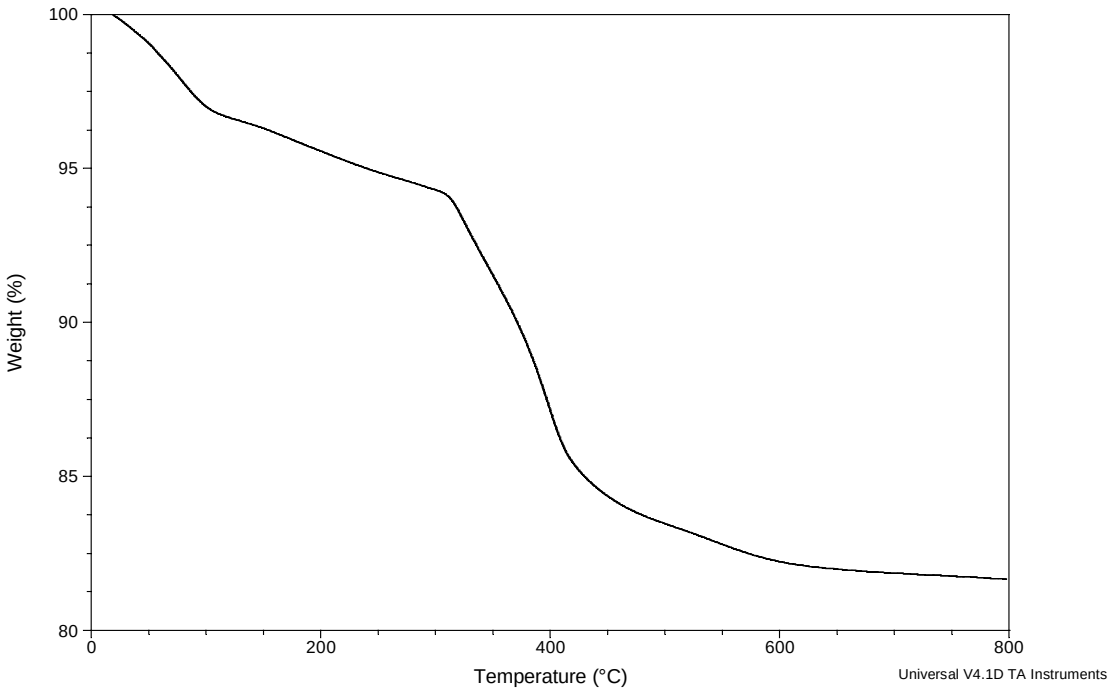

$[H_3N(CH_2)_4NH_3][V_4O_4(OH)_2\{O_3P(CH_2)_3PO_3\}_2]$•2.5H2O (4c·2.5$H_2O$)

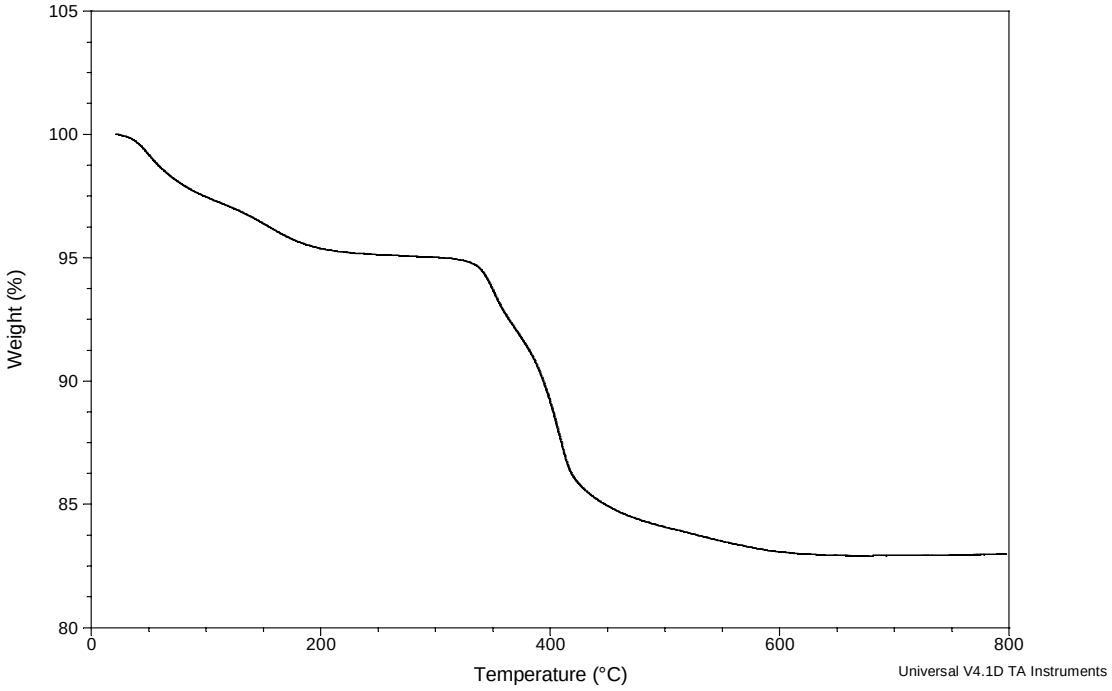

$[H_3N(CH_2)_5NH_3][V_4O_4(OH)_2\{O_3P(CH_2)_3PO_3\}_2]$•$H_2O$ (4d·H_2O)

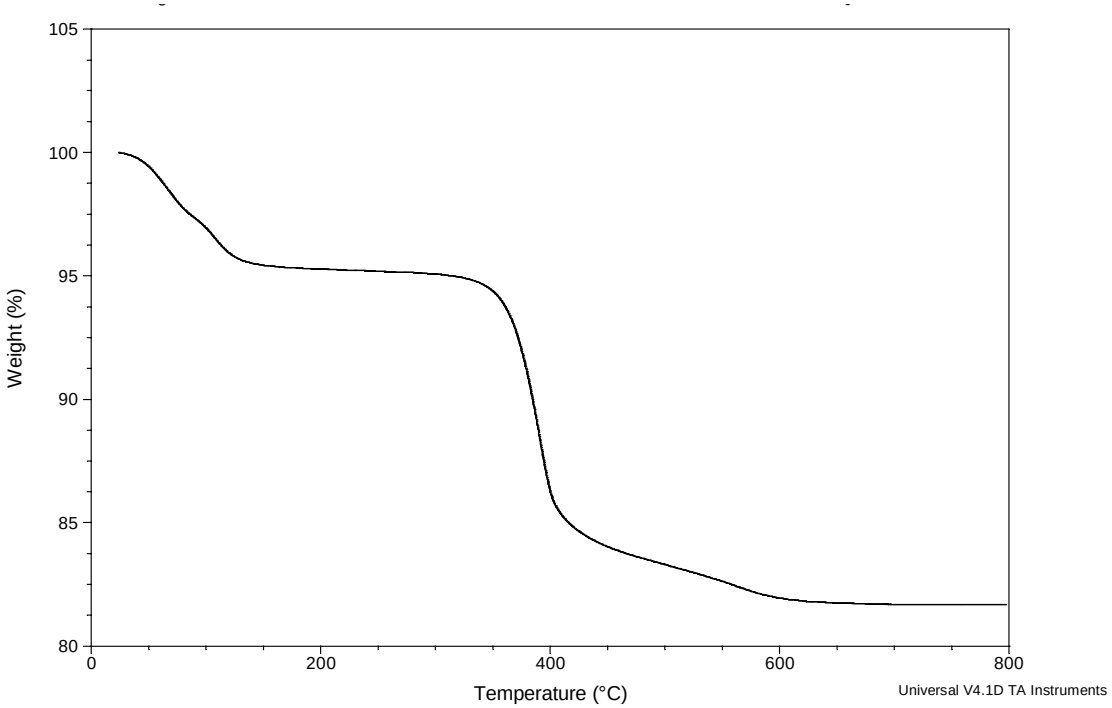

$[H_3N(CH_2)_6NH_3][\ [V_4O_4(OH)_2\{O_3P(CH_2)_3PO_3\}_2]\ ]\cdot 0.5H_2O$ (4e·0.5H_2O)

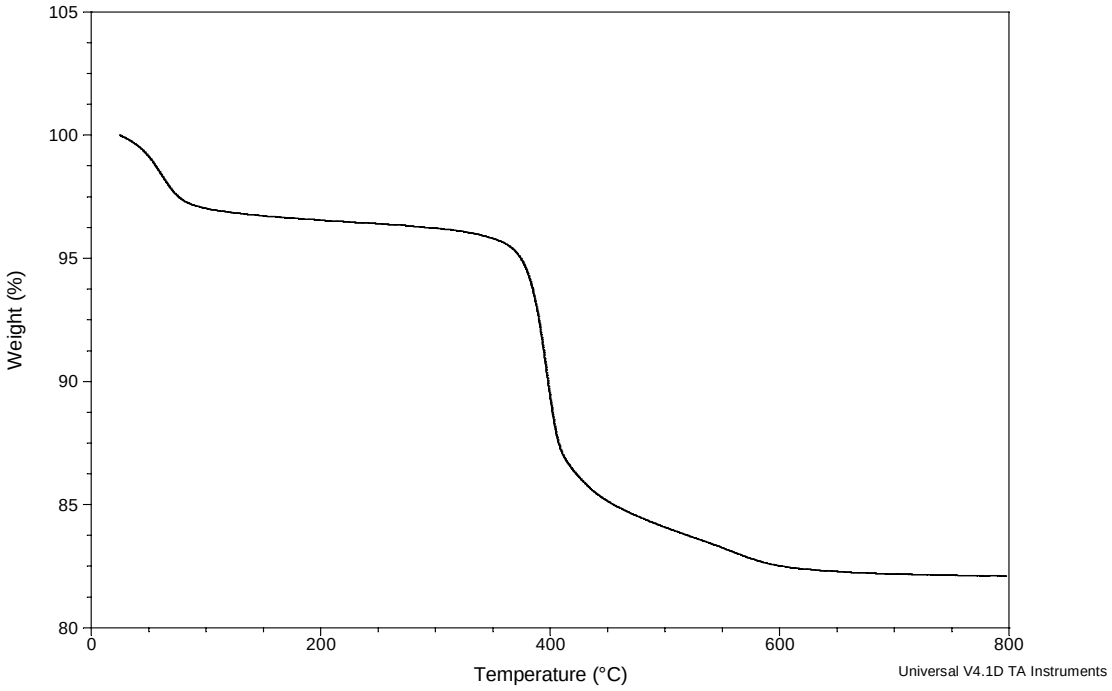

$[H_3N(CH_2)_7NH_3][V_4O_4(OH)_2\{O_3P(CH_2)_3PO_3\}_2]$ (4f)

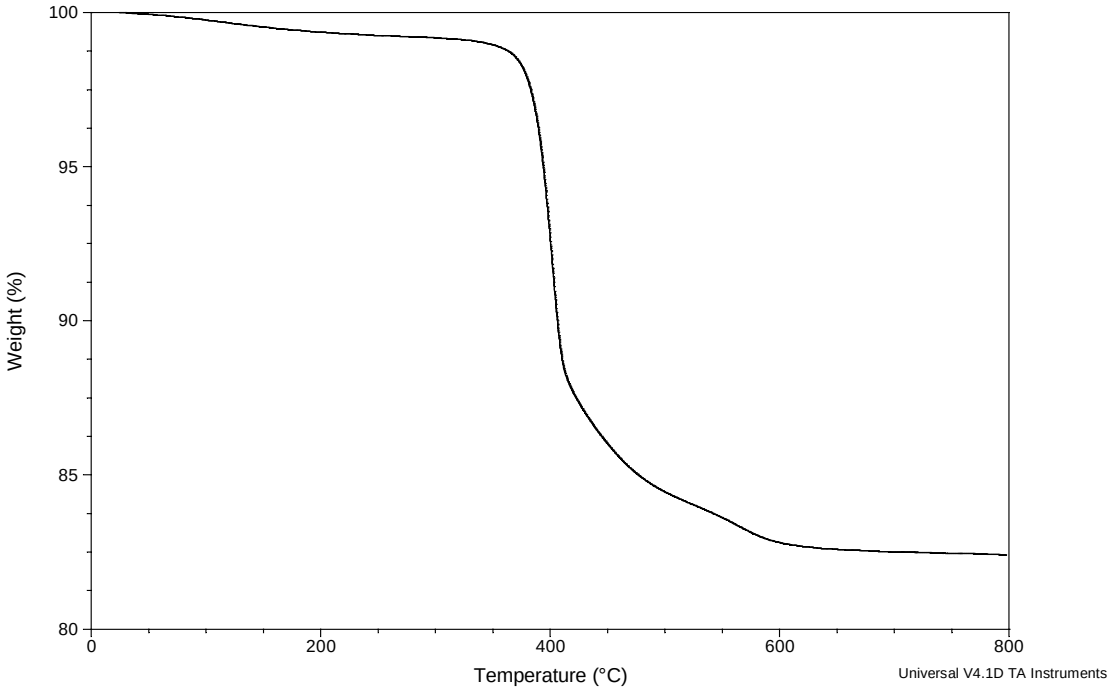

$[CH_3CH_2(NH_3)CH_2NH_3][V_4O_4(OH)_2\{O_3P(CH_2)_3PO_3\}_2]$ (4g)

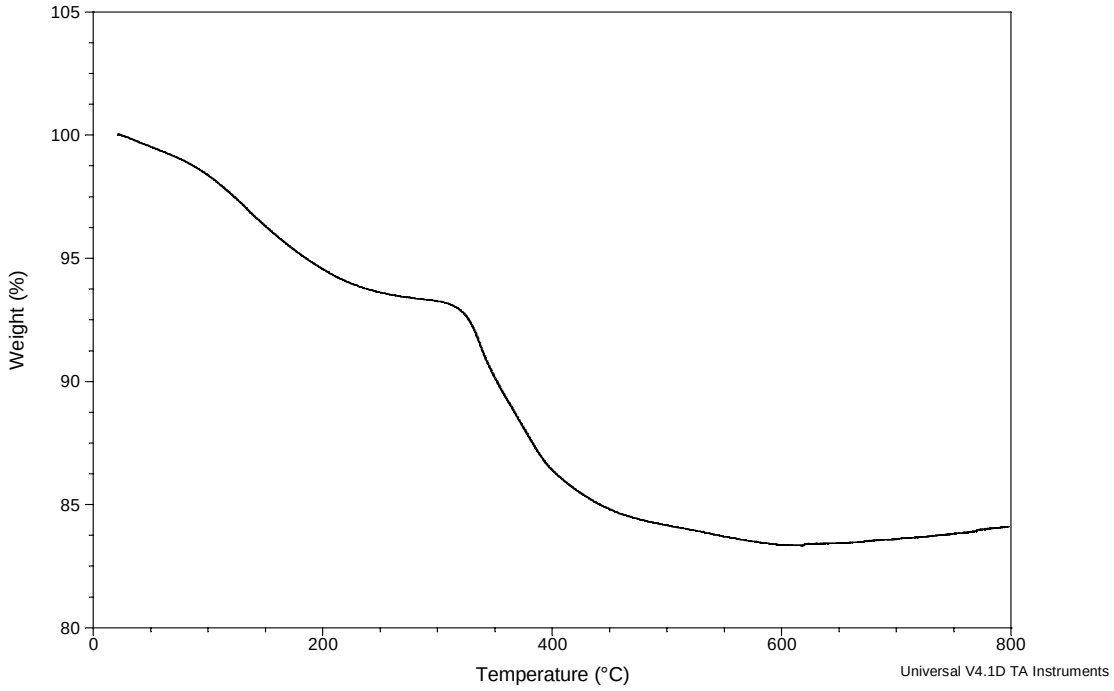

$[NH_3CH_3]_2[V_4O_4(OH)_2\{O_3P(CH_2)_3PO_3\}_2]\cdot 3H_2O$ (4h·$3H_2O$)

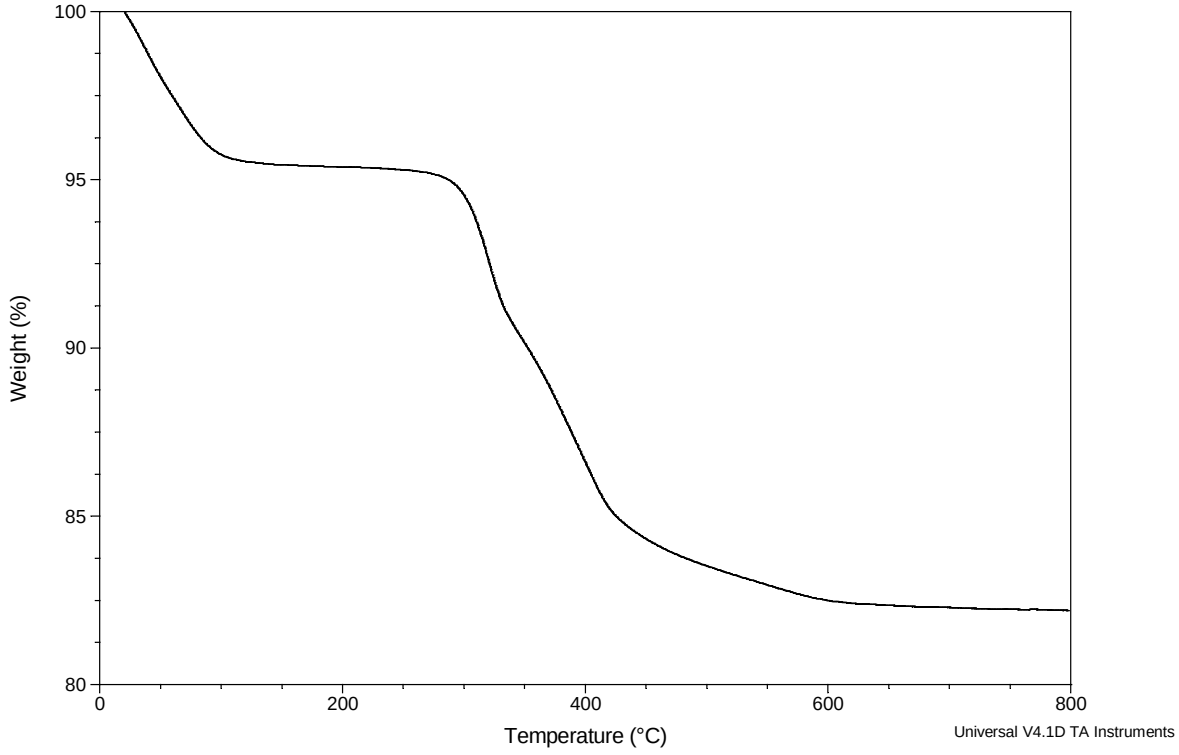

$[NH_3CH_2CH_2CH_3]_2[V_4O_4(OH)_2\{O_3P(CH_2)_3PO_3\}_2]$ (4j)

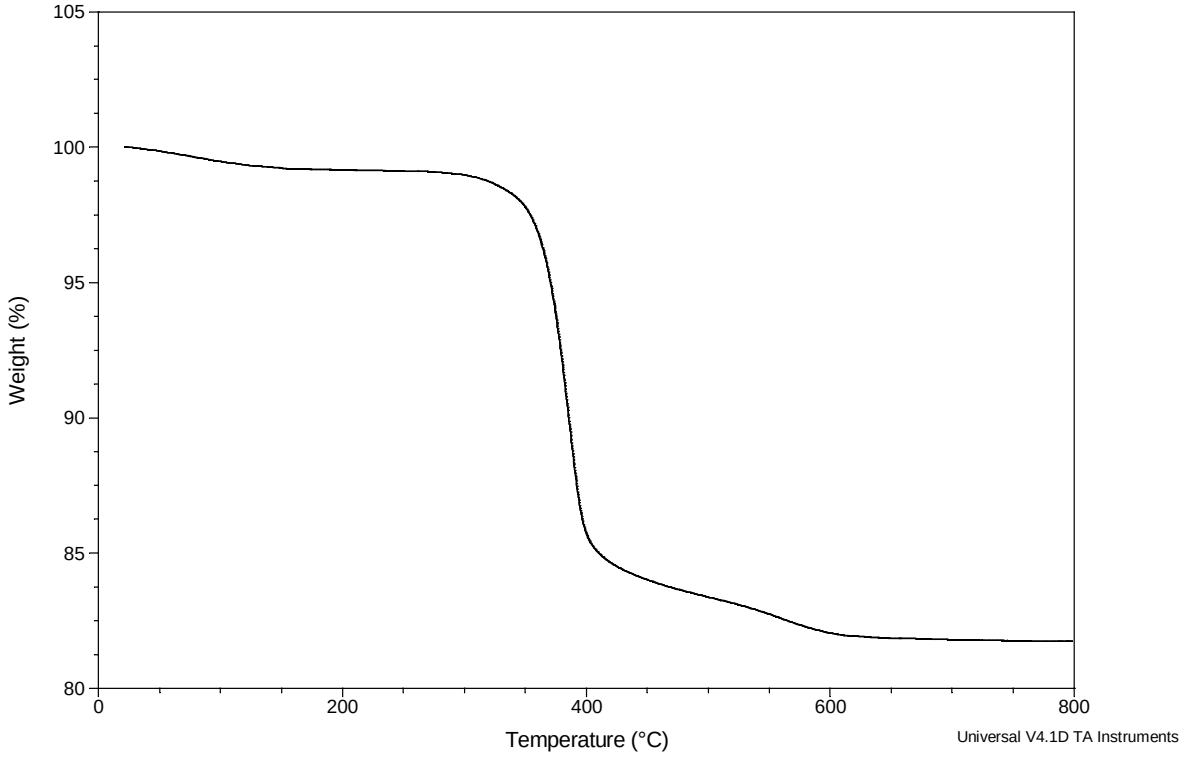

$[NH_2(CH_2CH_3)_2]_2[V_4O_4(OH)_2\{O_3P(CH_2)_3PO_3\}_2]\bullet 4H_2O$ (4k)

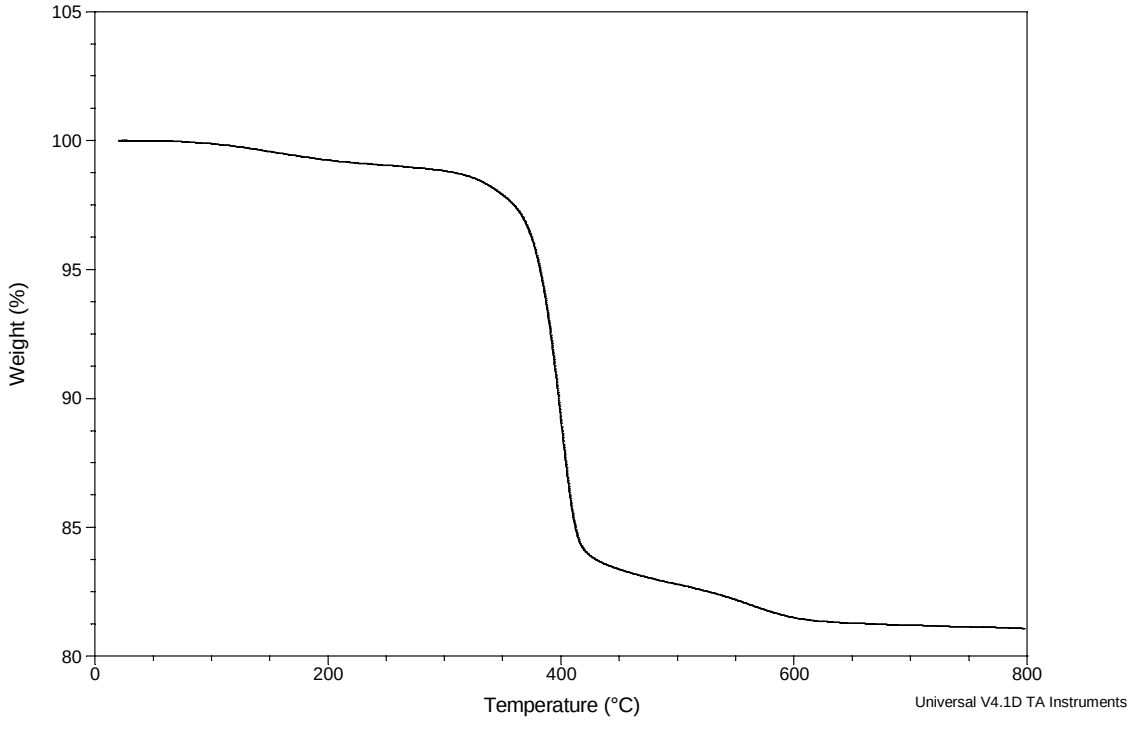

$[H_3N(CH_2)_2NH_3][V_4O_4(OH)_2\{O_3P(CH_2)_5PO_3\}_2]\cdot 0.75H_2O$ (5·0.75H_2O)

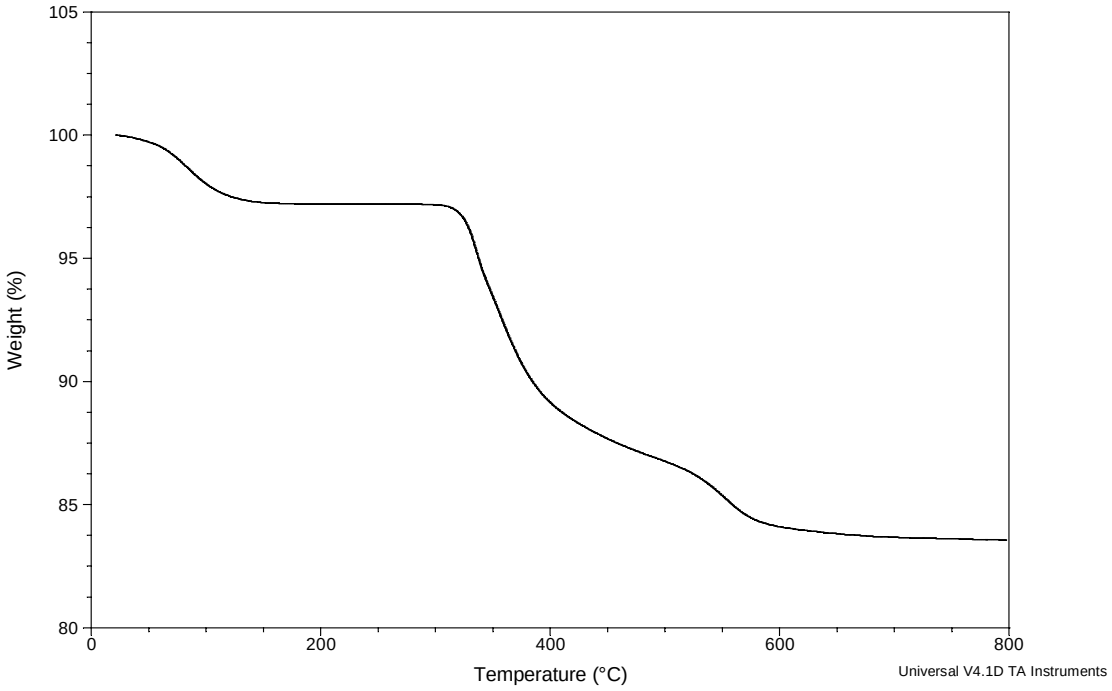

$[NH_2(CH_2CH_2)_2NH_2][V_2O_2\{HO_3P(CH_2)_2PO_3\}_2]$ (6a)

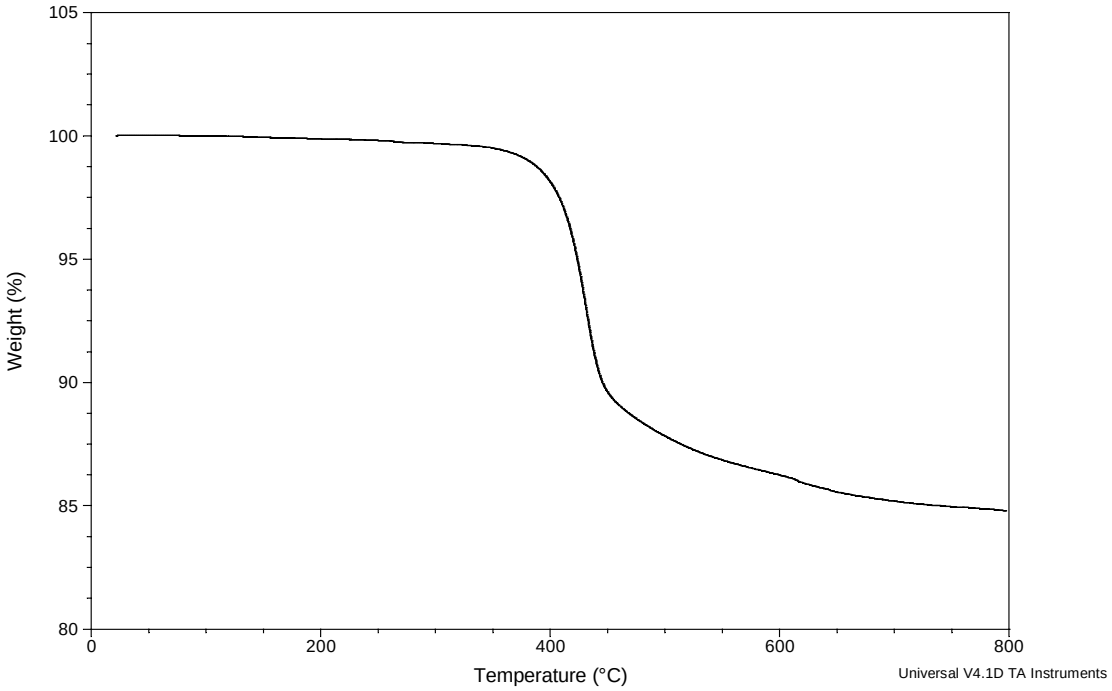

$[NH_2(CH_2CH_2)_2NH_2][V_2O_2\{HO_3P(CH_2)_4PO_3\}_2]$ (6b)

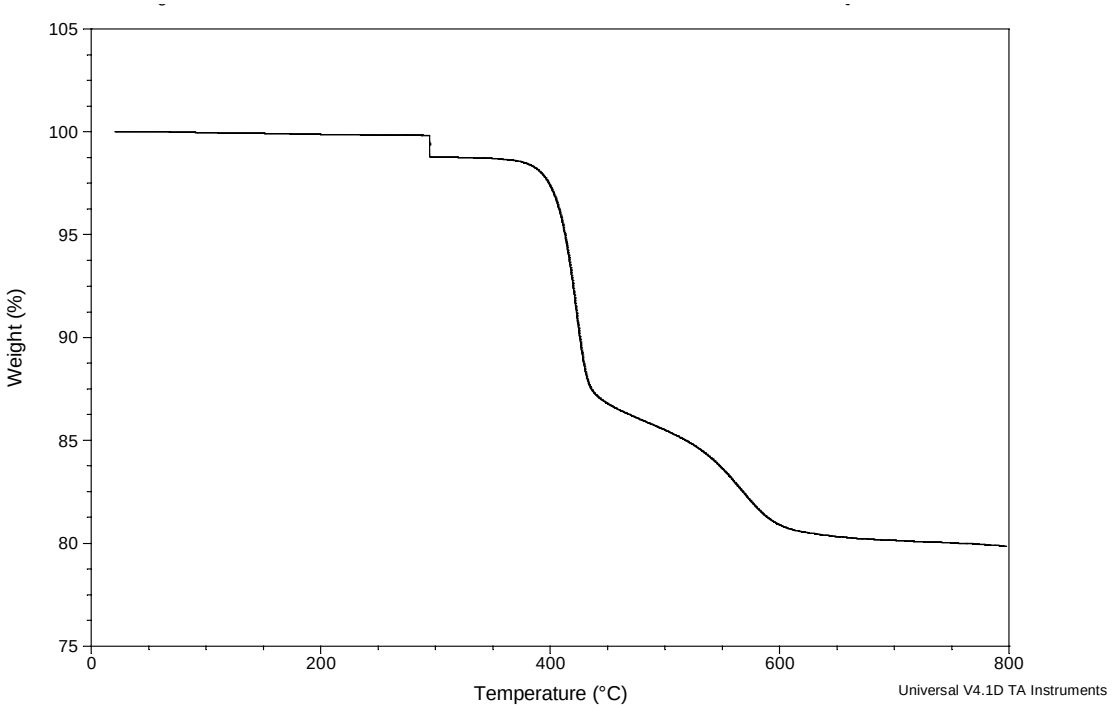

$[NH_2(CH_2CH_2)_2NH_2][V_2O_2\{HO_3P(CH_2)_6PO_3\}]$ (6c)

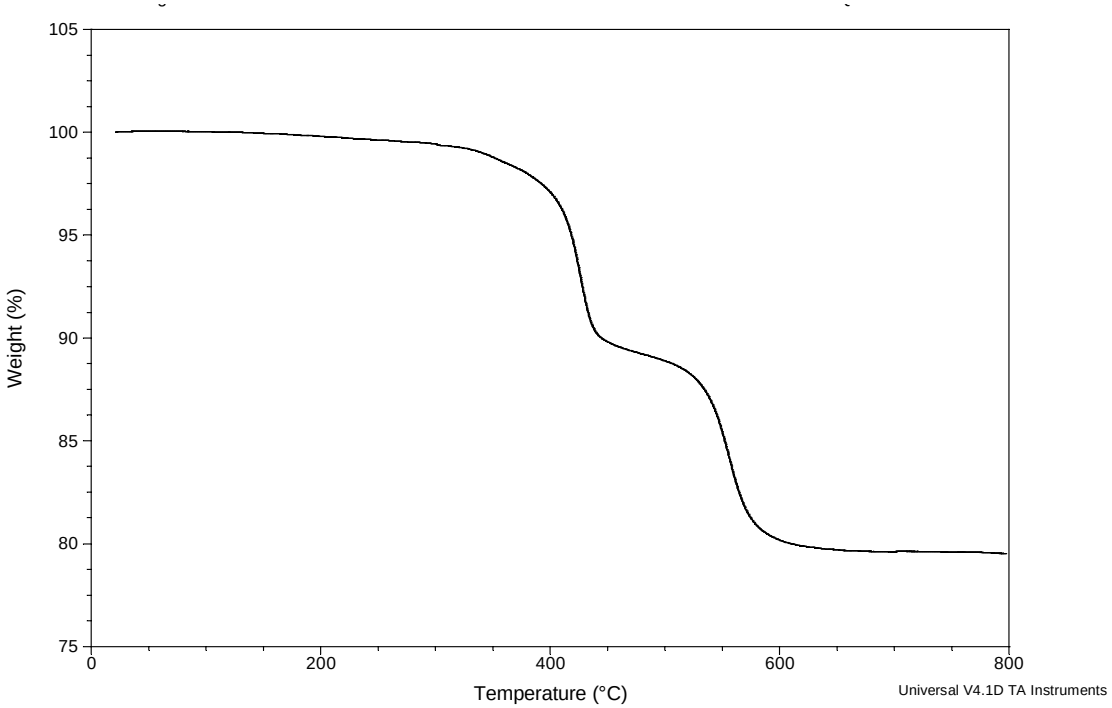

$[H_3N(CH_2)_5NH_3][(V_3O_3)\{O_3P(CH_2)_2PO_3\}_2]$ (7)

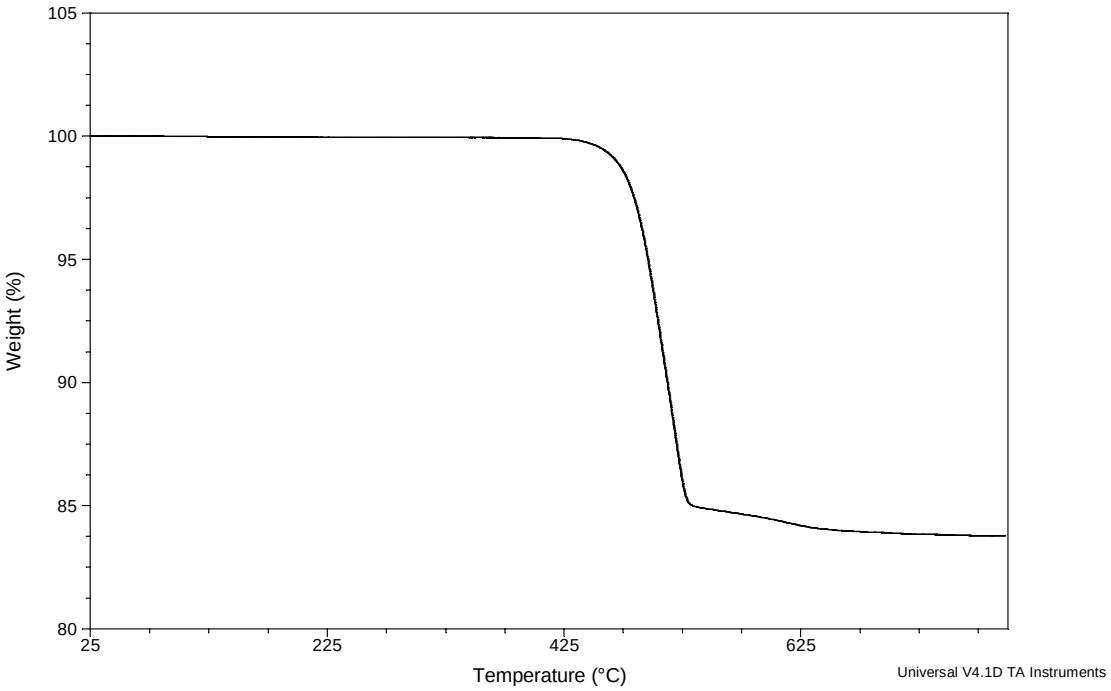
105
100
95
90
85
80
Weight (%)
25
225
425
625
Temperature (°C)
Universal V4.1D TA Instruments

IR spectra of **6c** and **6c'** (**6c** after heating to 426 °C for 3h).

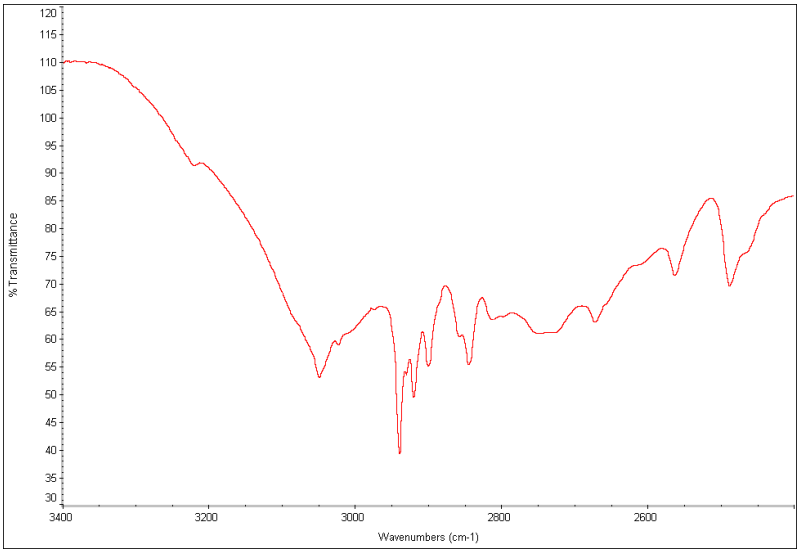

IR spectrum of **6c**.

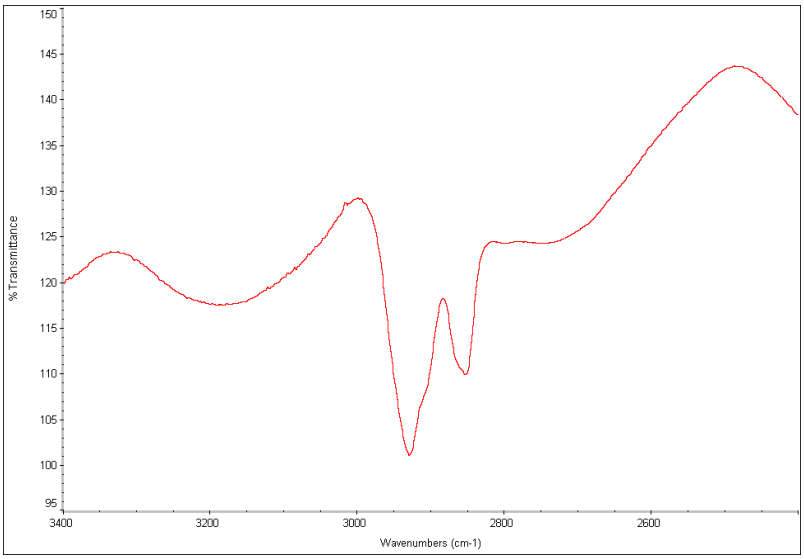

IR spectrum of **6c'**.

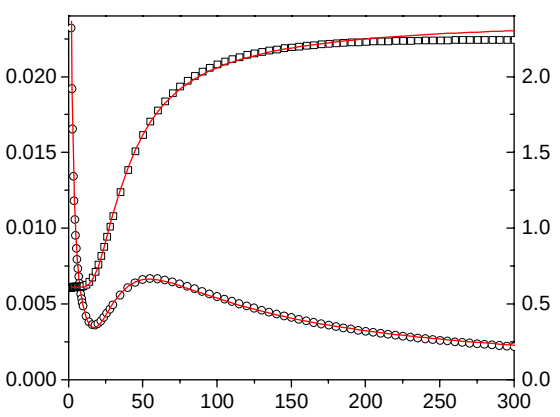

(a)

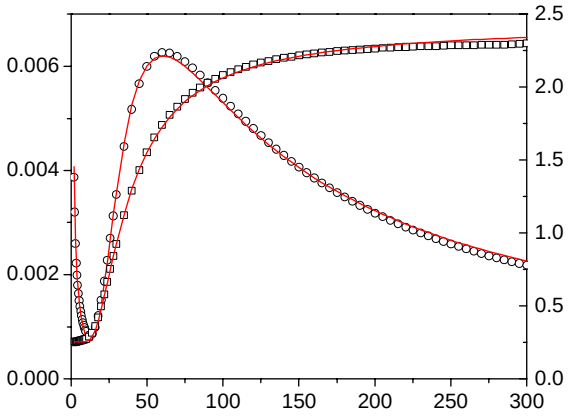

(b)

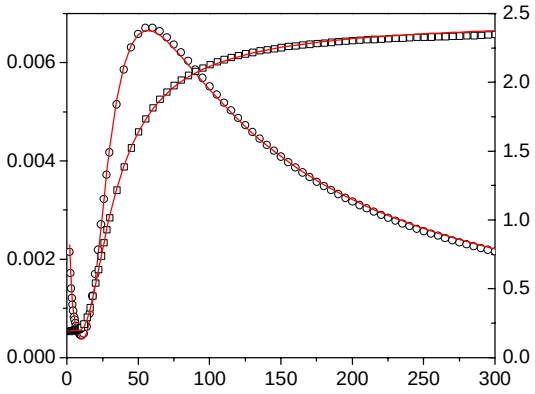

(c)

The dependence of the magnetic susceptibility χ (○) and the effective magnetic moment μ_{eff} (□) of (a) $[V_2O_2 (H_2O)\{O_3P(CH_2)_2PO_3\}]\bullet H_2O$ (1a), (b) $[V_2O_2 (H_2O)\{O_3P(CH_2)_4PO_3\}]\bullet 3H_2O$ (1c), (c) $[V_2O_2 (H_2O)\{O_3P(CH_2)_5PO_3\}]\bullet 3H_2O$ (1d) on the temperature T. The lines drawn through the data are the fits to the Heisenberg dimer model.

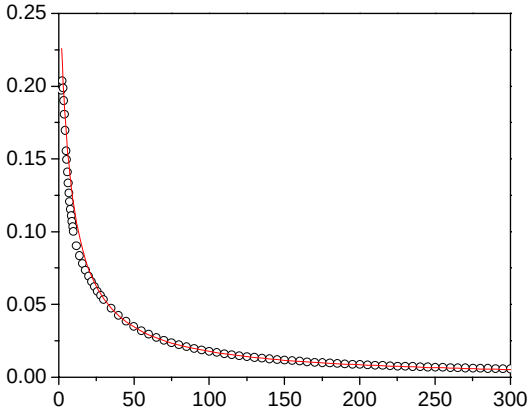

(a)

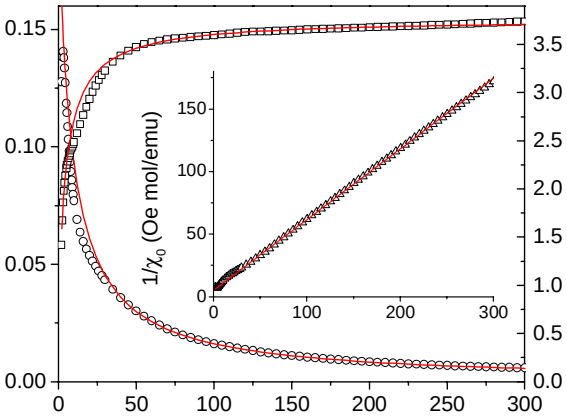

(b)

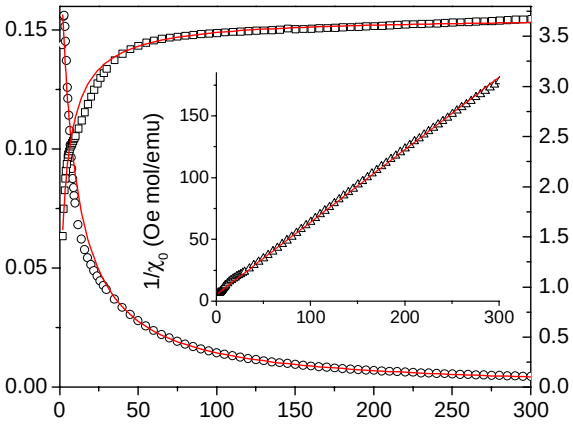

(c)

(a) The dependence of the magnetization M (○) of $[H_3N(CH_2)_2NH_3][V_4O_4(OH)_2\{O_3P(CH_2)_3PO_3\}_2]$ (4a) on the temperature T. The line drawn through the data is the fit to the Curie-Weiss law. The dependences of the magnetic susceptibility χ (○), the effective magnetic moment μ_{eff} (□) and the reverse susceptibility χ_0 (Δ) of (b) $[H_3N(CH_2)_3NH_3][V_4O_4(OH)_2\{O_3P(CH_2)_3PO_3\}_2]$ (4b) and $[H_3N(CH_2)_5NH_3][V_4O_4(OH)_2\{O_3P(CH_2)_3PO_3\}_2]$ (4d) on the temperature T. The lines drawn through the data are the fits to the Curie-Weiss law.

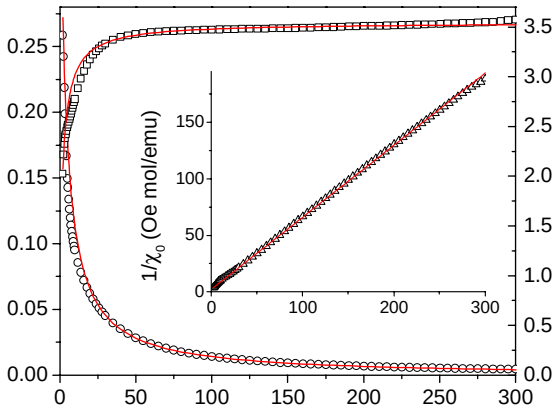

The dependence of the magnetic susceptibility χ (○), the effective magnetic moment μ_{eff} (□) and the reverse susceptibility χ_0 (Δ) of $[H_3N(CH_2)_2NH_3][V_4O_4(OH)_2(H_2O)\{O_3P(CH_2)_5PO_3\}_2]$ (5) on the temperature T. The lines drawn through the data are the fits to the Curie-Weiss law.

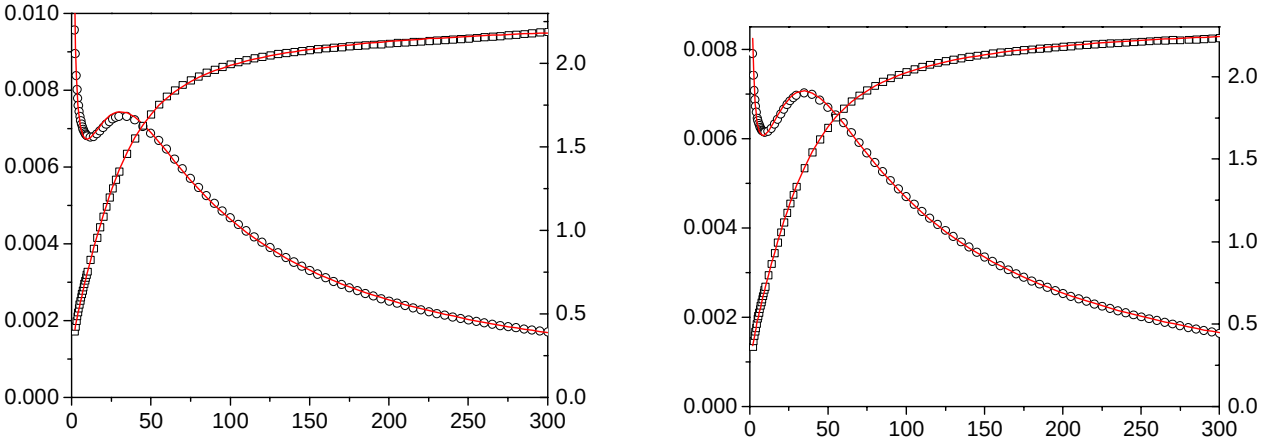

(a) (b)

The dependence of the magnetic susceptibility χ (○) and the effective magnetic moment μ_{eff} (□) of (a) $[H_2N(CH_2CH_2)_2NH_2][V_2O_2\{O_3P(CH_2)_2PO_3H\}_2]$ (6a) and (b) $[H_2N(CH_2CH_2)_2NH_2][V_2O_2\{O_3P(CH_2)_6PO_3H\}_2]$ (6c) on the temperature T. The lines drawn through the data are the fits to the Heisenberg linear AF chain model.

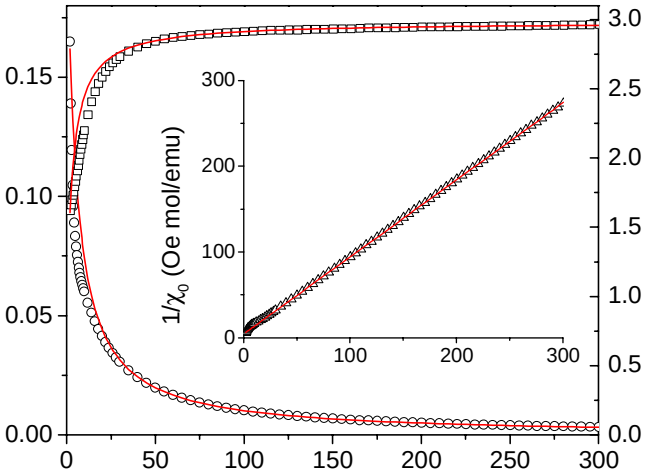

The dependence of the magnetic susceptibility χ (○), the effective magnetic moment μ_{eff} (□) and the reverse susceptibility χ_0 (Δ) of $[H_3N(CH_2)_5NH_3][V_3O_3\{O_3P(CH_2)_2PO_3\}_2]$ (7) on the temperature T. The lines drawn through the data are the fits to the Curie-Weiss law.